

Access this article online

Quick Response Code:



Website:

www.jorthodsci.org

DOI:

10.4103/jos.jos\_75\_24

# Debonding forces and failure modes of customized three-dimensional printed nano-ceramic hybrid resin fixed lingual retainers

Noor S. Alnuaimy and Akram F. Alhuwaizi

## Abstract

**BACKGROUND:** Retention preserves the optimal esthetic and functional positions of teeth following the termination of active orthodontic treatment. Conventional stainless-steel multistrand fixed retainers have limitations and drawbacks, mainly related to retainer failure.

**OBJECTIVES:** Nano-ceramic hybrid resin (SprintRay OnX) was employed to fabricate new, customized three-dimensional (3D)-printed lingual retainers, and their debonding forces and failure modes were evaluated.

**MATERIALS AND METHODS:** Pairs of premolars were embedded in acrylic blocks. Fifty acrylic blocks were divided into five groups, including three different cross-sections of customized 3D-printed wires— round (1 mm), oval (1 × 1.5 mm), and semi-elliptical (1 × 1.5 mm)— and comparative stainless steel multistrand retainers (G and H and Respond). Retainers were bonded to the teeth using Transbond™ LR Light Cure Adhesive. The models were stored in distilled water for 24 hours, simulating the wet intraoral conditions. Debonding forces and failure modes were then evaluated. A vertical debonding force was applied to the interdental area of the bonded retainer. Post-retainer debonding failure mode was examined under a stereomicroscope (×10 magnification).

**RESULTS:** Semi-elliptical 3D-printed retainers yielded the highest debonding forces, followed by oval 3D-printed retainers, twisted G and H retainers, round 3D-printed retainers, and Respond retainers. The debonding forces of oval and semi-elliptical 3D-printed retainers did not differ significantly. The 3D-printed retainer groups presented predominantly cohesive failure due to the strong adhesion between the 3D-printed resin and adhesive.

**CONCLUSION:** Oval and semi-elliptical 3D-printed retainers exhibited favorable debonding forces.

## Keywords:

3D-printed retainer, debonding, digital orthodontics, fixed lingual retainer, nanofiller

## Introduction

Post-orthodontic relapse is a complex, multifactorial condition exhibiting variability and unpredictability.<sup>[1]</sup> The optimal effective retention protocol and the ideal fixed retainer material and design are still debated. Conventional handcrafted stainless steel multistrand wire (MSW)

is the gold standard<sup>[2]</sup>; however, it has limitations and drawbacks mainly related to retainer failure, detrimental impact on periodontal health, unwanted tooth movements, and esthetic concerns.<sup>[3]</sup> In addition, a metal retainer must be removed before a magnetic resonance image (MRI)<sup>[4]</sup> and is contraindicated for metal allergies.<sup>[5]</sup>

Subtractive computer-aided design/ computer-aided manufacturing (CAD/ CAM) lingual retainers, including polyether

This is an open access journal, and articles are distributed under the terms of the Creative Commons Attribution-NonCommercial-ShareAlike 4.0 License, which allows others to remix, tweak, and build upon the work non-commercially, as long as appropriate credit is given and the new creations are licensed under the identical terms.

For reprints contact: WKHLRPMedknow\_reprints@wolterskluwer.com

**How to cite this article:** Alnuaimy NS, Alhuwaizi AF. Debonding forces and failure modes of customized three-dimensional printed nano-ceramic hybrid resin fixed lingual retainers. J Orthodont Sci 2025;14:2.

Department of  
Orthodontics, College of  
Dentistry, University of  
Baghdad, Baghdad, Iraq

## Address for correspondence:

Prof. Akram F. Alhuwaizi,  
Baghdad, Iraq.  
E-mail: akramalhuwaizi@  
codental.uobaghdad.  
edu.iq

Submitted: 13-Jul-2024

Revised: 11-Sep-2024

Accepted: 07-Nov-2024

Published: 25-Mar-2025

ether ketone (PEEK), nickel–titanium, zirconia, titanium, cobalt chromium, and fiber-reinforced composite, have emerged as a potential alternative to traditional MSWs.<sup>[2]</sup> Intraoral scanning and digital design offer a high degree of customization, imparting optimal placement, tighter interproximal adjustment, and enhanced fit accuracy in anatomically demanding situations.<sup>[6,7]</sup> Passive fitting is critical, as wire tension during bonding might cause unexpected teeth movements.<sup>[8]</sup> As 3D printing opens new perspectives, it exhibits superior performance compared to subtractive technologies, considering cost-effectiveness, minimal raw material waste, speed of manufacturing, and high-quality production of precise and complex geometries.<sup>[9]</sup> These attributes may augment the proposed advantages of subtractive CAD/CAM retainers.

A Cochrane Review,<sup>[10]</sup> systematic reviews and meta-analyses,<sup>[7,11]</sup> and some recent clinical studies<sup>[8,12,13]</sup> indicated no clinically significant differences in stability, periodontal health, survival, and failure rates between CAD/CAM and MSW retainers. Despite the new technology's appeal, CAD/CAM retainers did not seem more effective clinically compared to MSWs,<sup>[8]</sup> and they still possess certain drawbacks, including their bonding challenges<sup>[14–16]</sup> and high failure rates,<sup>[6]</sup> high cost and reliance on an external laboratory.<sup>[17]</sup> This study aimed to develop a novel customized 3D-printed lingual retainer using nano-ceramic hybrid resin, and the objectives were to measure the debonding forces and failure modes.

## Materials and Methods

### Pilot study

The pilot study evaluated the feasibility of employing the design and printing systems needed to produce lingual retainers with accurate cross-sectional geometries. A dental typodont model was scanned. Virtual drafts of nine customized retainers for each arch, including three samples of different cross-sections (round, oval, and semi-elliptical), were designed using Exocad Dental CAD software. The designs were optimized using Autodesk Meshmixer and 3D-printed according to the manufacturer's guidelines. The printed wire's cross-section was measured at six points: three mesiodistal midpoints of the crowns and three interdental midpoints. The printing quality was assessed by examining the wire's surface under a stereomicroscope ( $\times 10$  magnification). Two randomly allocated retainers (maxillary and mandibular) were bonded using Transbond™ LR Light Cure Adhesive [Figure 1].

### Specimen preparation

After acquiring ethical approval, a total of 135 human maxillary first premolars extracted for orthodontic purposes in private clinics from patients 15–30 years old

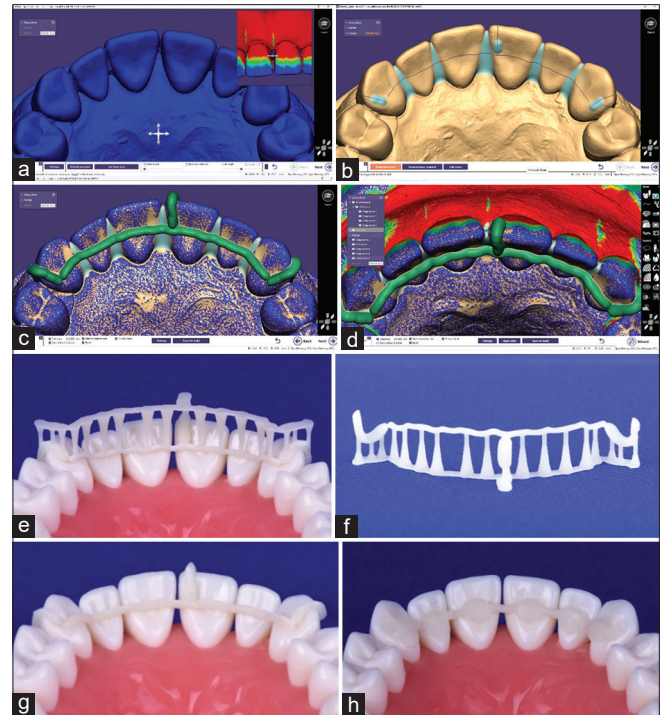


**Figure 1:** Lingual retainer fabrication: a, determining the insertion path; b, block-out the interdental area, wax-up the jigs' connection area and drawing the retainer; c and d, the designed retainer; e and f, the printed retainer; g, after supports' removal; and h, after bonding and jigs' removal

were collected. Teeth selection criteria included: intact lingual enamel surfaces free of cracks, caries, restorations, fluorosis, or anomalies, and no history of past bleaching, orthodontic, or endodontic treatments. The teeth were examined with a stereomicroscope ( $\times 10$  magnification) and blue light transillumination. Average-sized teeth (7–7.5 mm mesiodistal width and 22–23 mm length) were chosen. The selected teeth were kept at room temperature in a 0.1% thymol solution that changed weekly. Fifty teeth pairings were matched. Every tooth was trimmed less than 1 mm through one proximal side to simulate the intimate line contact between the anterior teeth.

Each teeth pair was mounted vertically in an acrylic block using a cylindrical plastic mold. The teeth were aligned by the surveyor's analyzing rod from the sides. Next, a custom-made T-shaped tool was attached to the surveyor to align the middle third of the lingual surfaces at the same level, parallel to the analyzing rod. Chemically cured acrylic resin was mixed and poured up to 2 mm apically to the cemento-enamel junctions' level. The blocks were stored in distilled water at room temperature until bonding.

Five groups of ten lingual retainers were prepared, including three groups of 3D-printed retainers constructed from nano-ceramic hybrid resin and two groups of MSW retainers that served as controls, as follows:

**Group I:** 1 mm diameter 3D-printed round customized lingual retainers (3D Round).

**Group II:** 1 mm thickness by 1.5 mm width 3D-printed oval customized lingual retainers (3D Oval).

**Group III:** 1 mm thickness by 1.5 mm width 3D-printed semi-elliptical customized lingual retainers (3D Semi-elliptical).

**Group IV:** 0.0195" twisted 7-strand stainless-steel retainers (G and H multistrand wire, G and H Orthodontics, Franklin, IN, USA; Twisted G and H).

**Group V:** 0.0195" dead-soft 6-strand coaxial stainless steel retainers (Respond Archwire, Ormco Corp., Orange, CA, USA; Coaxial Respond).

The mounted teeth of the three 3D-printed groups were digitized using a 3Shape TRIOS 3 intraoral scanner (3Shape, Copenhagen, Denmark) and exported as standard tessellation language (STL) files. The scanner was calibrated beforehand according to the manufacturer's guidelines. Exocad Dental CAD software was used to design customized lingual retainers with one of three cross-sectional geometries for each block [Figure 2]. The retainer was confirmed to be in contact with the middle of the lingual teeth surfaces and was well-adapted to the interdental areas. Just distal to the bonding locations, two attachment jigs, fitted to the lingual and occlusal surfaces, were designed to facilitate handling and precise seating. Earlier, the jigs' connection sites to the retainer were digitally waxed to facilitate their removal [Figure 3]. The design STL format was re-meshed using Autodesk Meshmixer software to create a denser triangulation, improving printing quality.

The 3D printing was executed with the Pro 95 Printer (SprintRay, Los Angeles, California, USA) and RayWare Automated Dental 3D Printing Software (version 2.9.1), following the manufacturer's guidelines. The samples were printed horizontally from the build platform to ensure consistent production without failure due to the wire's highly irregular and delicate nature, which precludes vertical printing. The printing supports were generated away from the fitting and bonding surfaces of the retainer with low density and 4 mm height for easy reduction. The nano-ceramic hybrid resin bottle (shade A1; SprintRay OnX, SprintRay, Los Angeles, California, USA; Lot S22C21XA1) was thoroughly mixed using an LC-3D Mixer before each print. The specimens were printed (50-micron-thick layer), left on the building board (5–10 min), washed (91% isopropyl alcohol spray), and then dried (compressed air) to remove any remaining uncured resin. Seven cleaning cycles were performed. Next, the sample was post-cured in the

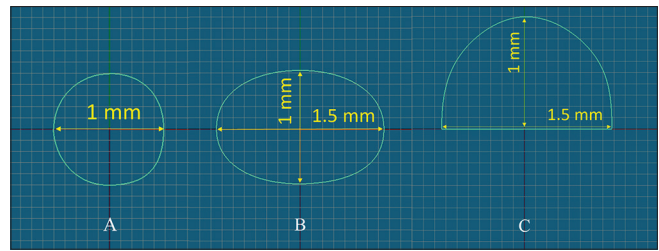


**Figure 2:** Drawing different cross-sections of the retainers by Exocad Dental CAD software: A, round; B, oval; and C, semi-elliptical

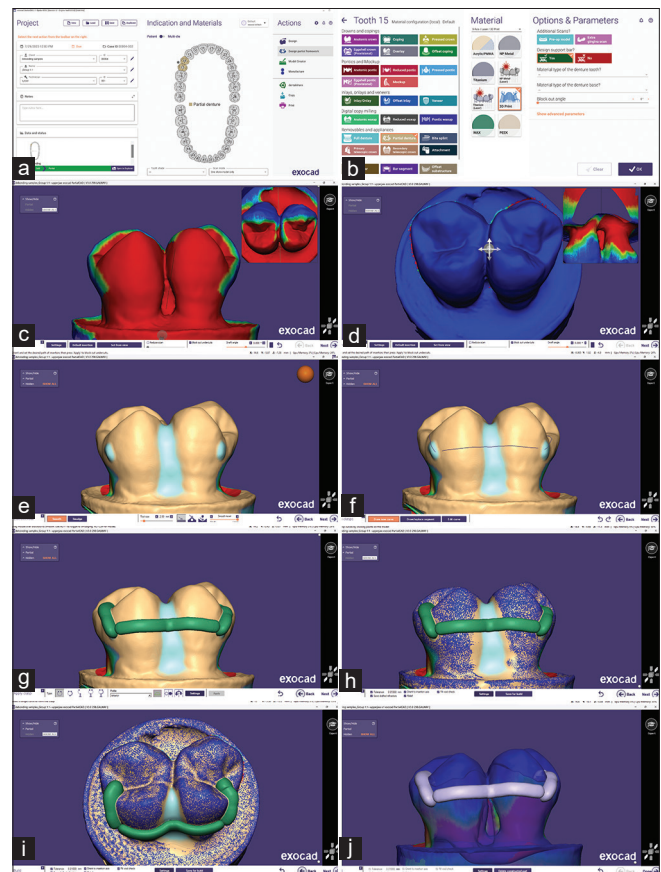


**Figure 3:** Designing 3D Oval: a and b, choosing the appliance and material types; c, loading the STL scan; d, determining the insertion path; e, block-out the interdental and wax-up the jigs' connection areas; f, drawing the retainer; g-i, the designed retainer; and j, STL file with transparent refractory

ProCure Post-Curing System (SprintRay, Los Angeles, California, USA), using a 90-watt LED array (365–405 nm wavelength and 28.8 mW/cm<sup>2</sup> light intensity) at 60°C for 60 min, to optimize their strength, accuracy, and thorough polymerization. The supports were then cut using a round diamond disk as near to the object as feasible [Figure 4a-c].

A stereomicroscope (×10 magnification) was utilized to analyze the wire's surface, determining its quality and ruling out any flaws or air bubbles. A digital caliper was used to measure the wire's dimensions to guarantee



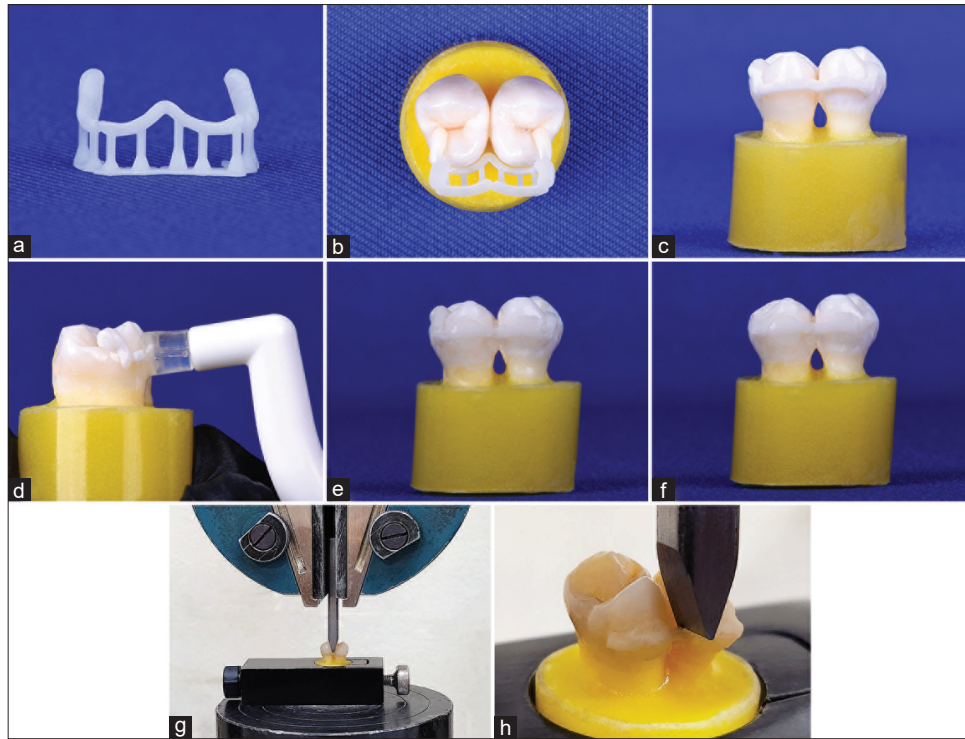


**Figure 4:** a and b, 3D-printed lingual retainer with supports; c, after removing supports; d, adhesive application on the center of premolars' lingual surface; e, bonded lingual retainer; f, after jigs' removal; g, debonding force test using Instron machine; and h, a close-up view

adequate printing accuracy. Samples containing defects were excluded.

The lengths of the two MSW groups were set at 15 mm. The retainer was adapted manually, by a gentle curve without bends, to fit passively on the middle third of the teeth's lingual surfaces, being as close as possible to the interdental area and parallel to the block base.

### Bonding procedure

The lingual surfaces of teeth were polished (10 s) with fluoride-free pumice and rubber cups, washed with water spray (10 s), and dried with oil-free air (10 s). They were then etched (30 s) with 37% phosphoric acid etching gel (Super-Etch, SDI, USA), washed thoroughly with water (20 s), and dried with compressed air (20 s) until the etched surface appeared chalky white.<sup>[18]</sup> Transbond™ LR Light Cure Adhesive (3M Unitek, Monrovia, California, USA) was used for the bonding procedure. A thin uniform primer coat (Transbond™ XT) was applied to the teeth surfaces using a disposable brush and then gently spread by an air jet (3 s). MSWs were placed such that the midpoint of the wire coincided with the interdental area; the printed retainers were seated on the teeth with jigs in place. A dome-shaped mold wire bonder (diameter 4 mm and depth 1.5 mm) was used to standardize the bonding pad's shape, area, and thickness and ensure that the wire was centered within the composite bond. The composite was light cured (10 s) according to

the manufacturer's instructions using 3M™ Elipar™ DeepCure-L (3M ESPE, Germany; 1470 mW/cm<sup>2</sup> light intensity) at approximately a 45° angle and 2 mm distance from the bonding surface. Subsequently, the jigs were removed carefully using a fine diamond fissure bur [Figure 4d-f].

### Debonding force test

After water storage of the bonded specimens at 37°C for 24 hours, debonding of the 50 blocks was conducted using a Tinius Olsen universal testing machine (H50KT, England) with a 50 kN load cell and a sensitivity of 2 N at ambient temperature. The sample was individually secured into a custom-made specimen-holding device attached to the lower jaw of the machine, while a custom-made plunger (1 mm diameter) was attached to the upper movable part. The specimen's long axis was parallel to the blade, and the chisel edge did not touch any part of the specimen. The crosshead exerted an occluso-lingual vertical load of 1 mm/min to the midpoint of the interdental segment, simulating the bite force. The load applied to the wire was gradually increased until debonding occurred on at least one premolar in the specimen [Figure 4g and h]. The maximum load for debonding (N) was recorded on a computer connected to the machine.

### Failure modes analysis

After the retainers' failure, two calibrated operators examined the wires and enamel surfaces under a

stereomicroscope ( $\times 10$  magnification). The investigator repeated the failure modes measurements after a one-month interval, and another operator evaluated the same samples. The Kappa test was used to ensure the intra-examiner and inter-examiner reliability, interpreted according to Landis and Koch<sup>[19]</sup> ratings, and showed a near-perfect agreement (0.97 for both).

The failure modes of both bonding sites were recorded, and the data of the one that failed first were analyzed. In cases where both bonds failed simultaneously, a lower score was recorded. The classification system was modified from that suggested by Foek *et al.*<sup>[20]</sup> as follows:

**Type 1:** Complete adhesive debonding from the tooth surface.

**Type 2:** Partial adhesive debonding from the tooth surface.

**Type 3:** The adhesive did not debond from the tooth surface, but the overlying adhesive on the retainer detached.

**Type 4:** The retainer did not debond from the tooth surface but fractured.

**Type 5:** The adhesive did not debond from the tooth surface, but the retainer dislodged.

### Statistical analyses

Statistical analyses were conducted using the Statistical Package for the Social Sciences (SPSS) software (version 25, IBM, USA) at a significance level of 0.05. Kappa scores assessed the reliability of failure modes. The Shapiro–Wilk normality test and Levene’s homogeneity test were applied to the debonding forces, revealing normally distributed data with equal variances; hence, one-way analysis of variance (ANOVA) and Tukey’s HSD *post hoc* tests were employed. The Kruskal–Wallis test was used to compare failure modes.

## Results

### Debonding force test

The 3D Semi-elliptical yielded the highest mean debonding forces, followed by the 3D Oval, Twisted G and H, 3D Round, and Coaxial Respond [Table 1]. According to Tukey’s HSD *post hoc* multiple comparisons, all intergroup comparisons had statistically significant differences in debonding forces, yet 3D Oval and 3D Semi-elliptical exhibited no significant differences.

### Failure modes

Predominantly, 3D-printed retainers demonstrated type 4 failure. Types 5, 3, and 2 were seen in Twisted G and H, whereas type 5 and 2 failures were observed in Coaxial Respond [Figure 5]. According to the Kruskal–



**Figure 5:** Representative specimens after debonding: a, 3D Round; b, 3D Oval; c, 3D Semi-elliptical; d, Twisted G and H; and e, Coaxial Respond

**Table 1: Descriptive and inferential statistics of the debonding forces (N) of 3D-printed retainers**

Groups	n	Mean	SD	Min	Max	ANOVA	Post Hoc Significance
3D Round	10	97.200	4.263	91.50	105.00	$F=725.399$ $df=49$ $P \leq 0.001^*$	All groups*
3D Oval	10	125.600	4.115	118.50	133.50		3D Round* Twisted G and H* Coaxial Respond*
3D Semi-elliptical	10	128.660	3.794	120.50	132.50		3D Round* Twisted G and H* Coaxial Respond*
Twisted G and H	10	115.050	2.510	111.00	118.50		All groups*
Coaxial Respond	10	57.750	1.550	54.50	59.50		All groups*

\*The difference is significant

**Table 2: Descriptive and inferential statistics of the failure modes of 3D-printed retainers**

Groups	n	Failure Modes					Kruskal–Wallis Statistics
		Type 1	Type 2	Type 3	Type 4	Type 5	
3D Round	10	0	1	0	9	0	$H=1.897$
3D Oval	10	0	2	0	8	0	$df=4$
3D Semi-elliptical	10	0	3	0	7	0	$P=0.755$
Twisted G and H	10	0	2	4	0	4	
Coaxial Respond	10	0	4	0	0	6	

Wallis test, the retainer type had no significant impact on the failure mode following debonding [Table 2].

## Discussion

Lingual retainers are supposed to function lifelong in the patient's mouth, which strains their durability.<sup>[2]</sup> Failure of the retainer results in a financial burden on the healthcare system and the patient, as the prior treatment is rendered ineffective, potentially necessitating retreatment. Water storage of specimens for 24 h at 37°C was the standard protocol before bond strength testing to simulate moisture and temperature conditions intraorally.<sup>[21,22]</sup> Increased orthodontic bond strength over the first 24 h was due to adhesive material maturation through additional polymerization.<sup>[23]</sup> Conversely, the most pronounced harmful impact of water absorption on the adhesive polymerization was within the initial 24-h. After that period, bond strength alterations are considered insignificant.<sup>[24]</sup> The debonding forces remain unaffected after that period or by various storage media used in the literature, including water, saline, and artificial saliva.<sup>[25]</sup> This study verifies the debonding forces and durability of the newly developed 3D-printed retainers after 24 h water storage.

The 3D printing makes it possible to design and produce any geometry; therefore, the 3D-printed wires were manufactured with various cross-sectional forms and a minimum thickness of 1 mm, which could be printed adequately with appropriate strength properties. For the patient's lingual comfort, rounded geometries on the lingual aspects of the retainers were adopted. Oval and semi-elliptical cross-sectional wires were aligned to have their greatest dimension along the teeth lingual surfaces, increasing the wire's strength and retention's surface area, but its thickness was kept to a minimum, providing a lower profile to avoid bulky constructions, thereby enhancing wire's flexibility and patient comfort.

Due to the composition similarity and the chemical nature of the adhesion between the polymethyl methacrylate (PMMA) 3D-printed resin and the adhesive composite, expectedly, the 3D-printed material possessed a more robust binding strength than MSWs, which rely

on mechanical retention. In parallel, the digital design permits bonding only in pre-planned optimal positions, ensuring better force distribution across the surfaces of the teeth. In this study, 3D Semi-elliptical and 3D Oval had flat designs, which increased their strength when subjected to bending forces across their larger dimensions. Given these assumptions, 3D Semi-elliptical yielded the highest debonding forces. Notably, despite the thinner composite bond (0.5 mm) of 3D-printed retainers, which did not comply with the optimum thickness (1 mm) proposed by Bearn *et al.*,<sup>[26]</sup> their bond was more robust than that of the MSWs. The 3D Semi-elliptical and 3D Oval had somewhat comparable values, neither statistically nor clinically significant, reflecting their comparable cross-sectional areas. In contrast, Coaxial Respond had the lowest debonding forces, which might be due to their dead-soft bending characteristics and elevated ductility resulting from the coaxial six-stranded configuration. Consistent with previous research,<sup>[27,28]</sup> the observed "V"-shaped deformations might suggest that the wire was dragged and deformed interdentally, resulting in high local stress, propagation of cracks, and retainer looseness and dislodgement.

The satisfactory clinical bond strength of orthodontic brackets must be 5.9–7.8 MPa.<sup>[29]</sup> However, this specification is meant to endure the forces generated by orthodontic appliances as well as the normal occlusal forces, while lingual retainers are just bonded passively. In addition, considerable force may be lost due to dissipation via the bonding sites and teeth.<sup>[30]</sup> Moreover, the 3D-printed retainer could be digitally designed entirely out of occlusion, reducing failure occurrence. Considering these concerns, a lower debonding threshold may be satisfactory for lingual retainers.<sup>[30]</sup> The limited information in the existing literature hinders the drawing of definitive conclusions.

The chemical bond between the 3D-printed wires and the composite was sufficiently strong to fortify the wire-composite complex. Incorporating nanofiller into 3D-printed resin might enhance the strength-to-mass ratio. Nevertheless, the wires exhibited unfavorable strength and relatively rigid behavior, suggesting that the stresses were more pronounced within the wire itself, contributing to a gradual stress buildup. This plausibly justifies that the predominant type of 3D-printed retainer failure was cohesive failure, while dislodgment of retainers was not observed, indicating high adhesive strength. The 3D Round showed lower debonding forces and the greatest incidence of type 4 failure due to the reduced cross-sectional area. No previous study has evaluated the failure mechanisms of 3D-printed retainers; however, in an earlier study, CAD/CAM PEEK retainers with and without optimization exhibited cohesive failure using similar interdental



vertical forces.<sup>[14]</sup> In contrast, despite no statistically significant differences in the failure modes concerning the retainer types, the MSWs were strong enough that none of them fractured during debonding; instead, type 2 failure was reported, as the wire-composite interface was the weakest point, which aligns with previous studies applying analogous methodologies.<sup>[14,27,28]</sup>

All failure modes in this study were advantageous, causing no direct damage to the enamel as does enamel-adhesive interface failure, though at the expense of extended chair time, increased cost, additional effort to remove the residual adhesive, and the use of rotary instruments (clean-up procedure) with potentially detrimental effects.<sup>[20]</sup> Interestingly, breaking 3D-printed wires before composite detachment might mitigate complications by facilitating the patient's detection so that treatment can be sought sooner.

The vertical interdental force employed in this study simulated the clinical bite, producing the highest shear forces compared to tensile forces.<sup>[31]</sup> Furthermore, applying force to the interdental segment ascertained the lowest debonding forces. These forces were expressed in Newtons rather than in Pascals because when a vertical force is applied to a bonded wire, complex multi-vectorial forces are produced simultaneously, i.e., tension, shear, and torsion forces.<sup>[27,32]</sup>

To the best of our knowledge, no previous research has assessed the debonding forces of 3D-printed retainers. In addition, the highly variable debond measurements in the existing literature were attributed to test configurations' multiplicity; therefore, this research is difficult to compare with previous studies. This study's findings should be interpreted cautiously due to the inherent inability of an *in vitro* study to replicate complex clinical conditions, such as the unavoidable use of premolars with variable morphology compared to the lingual surfaces of anterior teeth. Two teeth specimens might not accurately represent actual clinical forces dissipated across multiple bonding sites from canine to canine, resulting in a higher chance of clinical success.

Within the limits of this study, the emergence of a personalized 3D-printed lingual retainer can be considered in a dental clinical context. The 3D printing sector is constantly evolving. It offers the potential to tailor the material properties to specific clinical requirements. Improving the 3D-printed resin through composition modification or reinforcement can lead to better performance of the digital lingual retainer in the future.

## Conclusion

The cohesive failure associated with all 3D-printed

retainers indicated favorable adhesion yet less favorable strength. Oval and semi-elliptical 3D-printed retainers demonstrated favorable and comparable debonding forces despite consistent predominance of cohesive failure. Consequently, they might be suggested as an alternative to MSWs. However, long-term clinical trials are required.

## Key messages

The article provides insights into the performance of a nanofilled 3D-printed material fabricated as a 3D-printed lingual retainer in a novel orthodontic application, potentially paving the way for future investigation of the retainer.

## Ethical approval

This study was approved by the Research Ethics Committee-College of Dentistry/University of Baghdad (Reference no. 619 on 2-6-2022).

## Acknowledgments

The authors would like to gratefully thank Prof. Dr. Mohammed Nahidh Mohammed for statistical assistance.

## Financial support and sponsorship

Nil.

## Conflicts of interest

There are no conflicts of interest.

## References

1. Millett D. The rationale for orthodontic retention: Piecing together the jigsaw. *Br Dent J* 2021;230:739-49.
2. Roser CJ, Bauer C, Hodecker L, Zenthofer A, Lux CJ, Rues S. Comparison of six different CAD/CAM retainers vs. the stainless steel twistflex retainer: An *in vitro* investigation of survival rate and stability. *J Orofac Orthop* 2023;1-10.
3. Kartal Y, Kaya B, Polat-Ozsoy O. Comparative evaluation of periodontal effects and survival rates of Memotain and five-stranded bonded retainers: A prospective short-term study. *J Orofac Orthop* 2021;82:32-41.
4. Hasanin M, Kaplan SEF, Hohlen B, Lai C, Nagshabandi R, Zhu X, *et al.* Effects of orthodontic appliances on the diagnostic capability of magnetic resonance imaging in the head and neck region: A systematic review. *Int Orthod* 2019;17:403-14.
5. Kucera J, Littlewood SJ, Marek I. Fixed retention: Pitfalls and complications. *Br Dent J* 2021;230:703-8.
6. Jowett AC, Littlewood SJ, Hodge TM, Dhaliwal HK, Wu J. CAD/CAM nitinol bonded retainer versus a chairside rectangular-chain bonded retainer: A multicentre randomised controlled trial. *J Orthod* 2023;50:55-68.
7. Bardideh E, Ghorbani M, Shafaei H, Saeedi P, Younessian F. A comparison of CAD/CAM-based fixed retainers versus conventional fixed retainers in orthodontic patients: A systematic review and network meta-analysis. *Eur J Orthod* 2023;45:545-57.
8. Pullisaar H, Cattaneo PM, Gera A, Sankiewicz M, Bilinska M, Vandeveska-Radunovic V, *et al.* Stability, survival, patient satisfaction, and cost-minimization of CAD/CAM versus conventional multistranded fixed retainers in orthodontic

- patients: A 2-year follow-up of a two-centre randomized controlled trial. *Eur J Orthod* 2024;46:cjae006.
9. Panayi NC, Efstathiou S, Christopoulou I, Kotantoula G, Tsolakis IA. Digital orthodontics: Present and future. *AJO-DO Clin Companion* 2024;4:14-25.
10. Martin C, Littlewood SJ, Millett DT, Doubleday B, Bearn D, Worthington HV, *et al*. Retention procedures for stabilising tooth position after treatment with orthodontic braces. *Cochrane Database Syst Rev* 2023;5:CD002283.
11. Jedlinski M, Grocholewicz K, Mazur M, Janiszewska-Olszowska J. What causes failure of fixed orthodontic retention?-systematic review and meta-analysis of clinical studies. *Head Face Med* 2021;17:1-22.
12. Cokakoglu S, Adanur-Atmaca R, Cakir M, Ozturk F. Stability and failure rate during 3 years of fixed retention: A follow-up of an randomized clinical trial on adolescents with four different lingual retainers. *Orthod Craniofac Res* 2024;27:251-8.
13. Tran G, Rucker R, Foley P, Bankhead B, Adel SM, Kim KB. Relapse and failure rates between CAD/CAM and conventional fixed retainers: A 2-year follow-up of a randomized controlled clinical trial. *Eur J Orthod* 2024;46:cjad079.
14. Kadhum AS, Alhuwaizi AF. The efficacy of polyether-ether-ketone wire as a retainer following orthodontic treatment. *Clin Exp Dent Res* 2021;7:302-12.
15. Kadhum AS, Alhuwaizi AF. The effect of composite bonding spot size and location on the performance of poly-ether-ether-ketone (PEEK) retainer wires. *J Baghdad Coll Dent* 2021;33:1-9.
16. Ruwiae RA, Alhuwaizi AF. Effect of artificial aging test on PEEK CAD/CAM fabricated orthodontic fixed lingual retainer. *J Baghdad Coll Dent* 2022;34:1-6.
17. Gera A, Pullisaar H, Cattaneo PM, Gera S, Vandeyska-Radunovic V, Cornelis MA. Stability, survival, and patient satisfaction with CAD/CAM versus conventional multistranded fixed retainers in orthodontic patients: A 6-month follow-up of a two-centre randomized controlled clinical trial. *Eur J Orthod* 2023;45:58-67.
18. Ibrahim AI, Al-Hasani NR, Thompson VP, Deb S. Resistance of bonded premolars to four artificial ageing models post enamel conditioning with a novel calcium-phosphate paste. *J Clin Exp Dent* 2020;12:e317-26.
19. Landis JR, Koch GG. The measurement of observer agreement for categorical data. *Biometrics* 1977;33:159-74.
20. Foek DL, Yetkiner E, Ozcan M. Fatigue resistance, debonding force, and failure type of fiber-reinforced composite, polyethylene ribbon-reinforced, and braided stainless steel wire lingual retainers *in vitro*. *Korean J Orthod* 2013;43:186-92.
21. Garma NMH, Ibrahim AI. Development of a remineralizing calcium phosphate nanoparticle-containing self-etching system for orthodontic bonding. *Clin Oral Investig* 2023;27:1483-97.
22. Kadhim HA, Deb S, Ibrahim AI. Performance of novel enamel-conditioning calcium-phosphate pastes for orthodontic bonding: An *in vitro* study. *J Clin Exp Dent* 2023;15:e102-9.
23. Vinagre AR, Messias AL, Gomes MA, Costa AL, Ramos JC. Effect of time on shear bond strength of four orthodontic adhesive systems. *Rev Port Estomatol Cir Maxilofac* 2014;55:142-51.
24. Takamizawa T, Barkmeier WW, Tsujimoto A, Scheidel DD, Watanabe H, Erickson RL, *et al*. Influence of water storage on fatigue strength of self-etch adhesives. *J Dent* 2015;43:1416-27.
25. Nirupama C, Kavitha S, Jacob J, Balaji K, Srinivasan B, Murugesan R, *et al*. Comparison of shear bond strength of hydrophilic bonding materials: An *in vitro* study. *J Contemp Dent Pract* 2012;13:637-43.
26. Bearn DR, McCabe JF, Gordon PH, Aird JC. Bonded orthodontic retainers: The wire-composite interface. *Am J Orthod Dentofacial Orthop* 1997;111:67-74.
27. Baysal A, Uysal T, Gul N, Alan MB, Ramoglu SI. Comparison of three different orthodontic wires for bonded lingual retainer fabrication. *Korean J Orthod* 2012;42:39-46.
28. Lee IH, Lee JH, Park IY, Kim JH, Ahn JH. The effect of bonded resin surface area on the detachment force of lingual bonded fixed retainers: An *in vitro* study. *Korean J Orthod* 2014;44:20-27.
29. Reynolds IR. A review of direct orthodontic bonding. *Br J Orthod* 2016;2:171-8.
30. Golshah A, Feyli SA. Bond strength and deflection of four types of bonded lingual retainers. *Int J Dent* 2022;2022:1-7.
31. Reicheneder C, Hofrichter B, Faltermeier A, Proff P, Lippold C, Kirschneck C. Shear bond strength of different retainer wires and bonding adhesives in consideration of the pretreatment process. *Head Face Med* 2014;10:51.
32. Cooke ME, Sherriff M. Debonding force and deformation of two multi-stranded lingual retainer wires bonded to incisor enamel: An *in vitro* study. *Eur J Orthod* 2010;32:741-6.